
ViDA: Homeostatic Visual Domain Adapter for Continual Test Time Adaptation

Jiaming Liu^{1*}, Senqiao Yang^{1*}, Peidong Jia¹,
Ming Lu¹, Yandong Guo², Wei Xue³, Shanghang Zhang^{1†}

¹National Key Laboratory for Multimedia Information Processing,
School of Computer Science, Peking University

²AI2Robotics ³ Hong Kong University of Science and Technology

Abstract

Since real-world machine systems are running in non-stationary and continually changing environments, Continual Test-Time Adaptation (CTTA) task is proposed to adapt the pre-trained model to continually changing target domains. Recently, existing methods mainly focus on model-based adaptation, which aims to leverage a self-training manner to extract the target domain knowledge. However, pseudo labels can be noisy and the updated model parameters are uncertain under dynamic data distributions, leading to error accumulation and catastrophic forgetting in the continual adaptation process. To tackle these challenges and maintain the model plasticity, we tactfully design a Visual Domain Adapter (ViDA) for CTTA, explicitly handling both domain-specific and domain-agnostic knowledge. Specifically, we first comprehensively explore the different domain representations of the adapters with trainable high and low-rank embedding space. Then we inject ViDAs into the pre-trained model, which leverages high-rank and low-rank prototypes to adapt the current domain distribution and maintain the continual domain-shared knowledge, respectively. To adapt to the various distribution shifts of each sample in target domains, we further propose a Homeostatic Knowledge Allotment (HKA) strategy, which adaptively merges knowledge from each ViDA with different rank prototypes. Extensive experiments conducted on four widely-used benchmarks demonstrate that our proposed method achieves state-of-the-art performance in both classification and segmentation CTTA tasks. In addition, our method can be regarded as a novel transfer paradigm and showcases promising results in zero-shot adaptation of foundation models to continual downstream tasks and distributions.

1 Introduction

Deep Neural Networks (DNN) have achieved remarkable performance in various computer vision tasks, such as classification [23, 15], object detection [49, 66], and segmentation [10, 60], when the test data distribution is similar to the training data. However, real-world machine perception systems (i.e., autonomous driving [1, 29]) operate in non-stationary and constantly changing environments, which contain heterogeneous and dynamic domain distribution shifts. Applying a pre-trained model in these real-world tasks [51] can lead to significant degradation in perception ability on target domains, especially when the target distribution changes unexpectedly over time. Therefore, developing continual domain adaptation (DA) methods that can enhance the generalization capability of DNNs and improve the reliability of machine perception systems in dynamic environments.

*Equal contribution: liujiaming@bupt.edu.cn

†Corresponding author: shzhang.pku@gmail.com

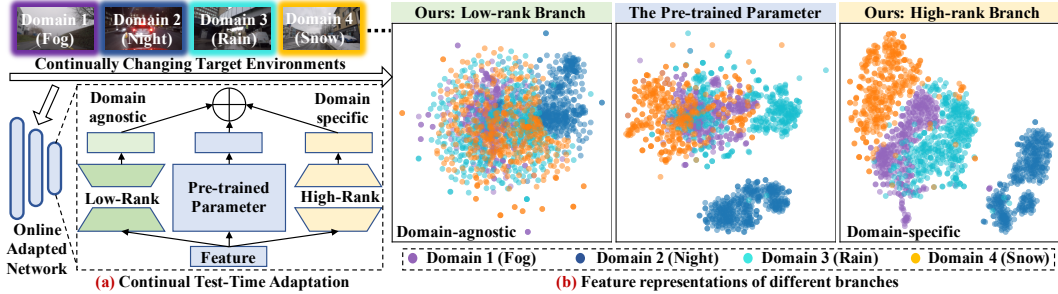


Figure 1: **The problem and motivation of our method.** (a) Our goal is to effectively adapt the source pre-trained model to continually changing target domains. We propose Visual Domain Adapters with different domain representations to tackle the error accumulation and catastrophic forgetting challenges during the continual adaptation process. We leverage ViDAs with high-rank and low-rank prototypes to adapt current domain distribution and maintain the continual domain-agnostic knowledge, respectively. (b) we conduct a t-SNE [55] analysis for the different adapter distributions across four target domains (ACDC). The low-rank branch exhibits a consistent distribution across the target domains, suggesting that it can effectively disregard the impact of dynamic distribution shifts. The high-rank branch demonstrates noticeable distribution discrepancies between the various target domains, suggesting that it primarily focuses on extracting domain-specific knowledge.

A classical source-free DA task, Test-Time Adaptation [40] (TTA), eases the distribution shift between a source domain and a fixed target domain. This is typically achieved through the utilization of self-training mechanisms [43, 57]. However, when adapting to continually changing target domains, pseudo labels are noisy and the updated model parameters become uncertain, leading to error accumulation and catastrophic forgetting. To tackle this problem, Continual Test-Time Adaptation (CTTA) has been proposed [59], which addresses a sequence of different distribution shifts over time rather than a single shift as in TTA. Furthermore, CTTA also encompasses the efficient zero-shot adaptation of foundation models to continual downstream tasks or distributions [2, 30].

Existing CTTA works [59, 8, 17, 61] have primarily employed model-based and prompt-based approaches to extract target domain-specific and domain-invariant knowledge simultaneously. However, for model-based methods [59, 8], the noisy pseudo labels are still unreliable and play a limited role in avoiding error accumulation, particularly in scenarios with significant distribution gaps. Meanwhile, prompt-based methods [17, 61] face difficulties in leveraging soft prompts with limited trainable parameters to learn long-term domain-shared knowledge and prevent catastrophic forgetting.

To tackle these limitations and maintain the model plasticity, we tactfully design a homeostatic Visual Domain Adapter (ViDA), shown in Fig. 1 (a), which explicitly manages domain-specific and domain-agnostic knowledge in the continual adaptation process. Specifically, we first carefully explore the different domain representations of ViDAs with trainable high and low-rank embedding space. Our observations reveal that ViDA with a low-rank prototype focuses on domain-agnostic feature representation in different domains. As shown in Fig. 1 (b), the prototype distribution of the adapter neglects the influence of dynamic distribution shifts. Conversely, ViDA with a high-rank prototype concentrates more on extracting domain-specific knowledge, as evidenced by the prototype distribution in different target domains showing an obvious discrepancy. We provide a detailed explanation of the motivations in Section 3.1.

This observation motivates us to inject ViDAs into the pre-trained model, which leverages high and low-dimension prototype to adapt current domain distribution and maintain the continual domain-shared knowledge, respectively. According to the various distribution shift of each sample, we further propose a Homeostatic Knowledge Allotment (HKA) strategy to dynamically fuse the knowledge from each ViDA with different dimension prototypes. In Fig. 1 (b), HKA adaptively regularizes the balance of different feature representations, including original model, domain-specific, and domain-agnostic features. During inference, the different domain-represented ViDAs can be projected into the pre-trained model by re-parameterization [14], which ensures no extra parameter increase and maintain the model plasticity. In addition, through the proposed homeostatic ViDAs, we empower the model with domain generalization ability, which achieves a significant improvement (+7.6%) on the five unseen target domains of ImageNet-C. In summary, our contributions are as follows:

- We carefully study the different domain representations of the adapters with high and low-rank prototypes. And we tactfully design a Visual Domain Adapter (ViDA) for CTTA, explicitly managing domain-specific and domain-shared knowledge to tackle the error accumulation and catastrophic forgetting problem, respectively.
- According to the various distribution shift of each sample in the target domains, we further propose a Homeostatic Knowledge Allotment (HKA) strategy to dynamically fuse the knowledge from each ViDA with different rank prototypes.
- Our proposed approach outperforms most state-of-the-art methods according to the experiments on four benchmark datasets, covering classification and segmentation tasks.
- Our CTTA method provides a novel transfer paradigm and achieves a promising result in zero-shot adapting of foundation models to continual downstream distributions. Meanwhile, we empower the source model with domain generalization ability through the proposed homeostatic ViDAs, achieving a significant improvement on the unseen target domains.

2 Related work

2.1 Continual Test-Time Adaptation

Test-time adaptation (TTA), also referred to as source-free domain adaptation [6, 35, 41, 62], aims to adapt a source model to an unknown target domain distribution without relying on any source domain data. Recent research has explored self-training and entropy regularization techniques to fine-tune the source model [36, 58, 41, 9]. Tent [58] updates the training parameters in batch normalization layers by minimizing entropy. Recently, there has been a surge of interest in performing Transformer-based TTA works [59, 21, 21]. **Continual Test-Time Adaptation (CTTA)** refers to a scenario where the target domain is not static, presenting additional challenges for traditional TTA methods. The first approach to address this challenging task is introduced in [59], which combines bi-average pseudo labels and stochastic weight reset. While [59, 8] tackles the problem in both classification and segmentation tasks at the model level, [17] introduces the use of visual domain prompts to address the issue at the input level specifically for the classification task. In this paper, we simultaneously focus on both classification tasks and dense prediction tasks.

2.2 Parameter-Efficient Fine-Tuning

Recently, Parameter-Efficient Fine-Tuning (PEFT) has gained significant traction within the field of natural language processing (NLP) [31, 27, 26, 64, 38, 28, 20, 24, 56, 46]. Adapter-based models, a form of PEFT, have gained popularity in NLP. They employ bottleneck architecture adapter modules inserted between layers in pre-trained models. During fine-tuning, only these modules are updated. Adapter-based models demonstrate dominant performance over other methods in certain tasks, sometimes surpassing standard fine-tuning [13]. Inspired by NLP, adapters in visual tasks have also received widespread attention. In the initial phases of adapter development, residual adapter modules [47, 48] are proposed to aid in the effective adaptation of convolutional neural networks across multiple downstream tasks. AdaptFormer [11] enhances the ViT [15] model by replacing the original multi-layer perceptron (MLP) block with AdaptMLP. AdaptMLP introduces a trainable down-to-up bottleneck module in a parallel manner, effectively mitigating catastrophic interference between tasks. VL-Adapter [53] improves the efficiency and performance of adapters by sharing low-dimensional layers weights to attain knowledge across tasks. Existing methods, as mentioned, have not addressed the challenges of long-term preservation of domain-agnostic knowledge and timely exploration of domain-specific knowledge amidst continuous unknown domain variations. Consequently, there is an urgent demand for an adapter with different domain representations that can simultaneously tackle the challenges of error accumulation and catastrophic forgetting.

3 Method

In Continual Test-Time Adaptation (CTTA), we pre-train the model $q_\theta(y|x)$ on the source domain $D_S = (Y_S, X_S)$ and adapt it on multiple target domains $D_{T_i} = \{(X_{T_i})\}_{i=1}^n$, where n represents the scale of the continual target datasets. The entire process can not access any source domain data and can only access target domain data once. The distributions of the target domains (i.e.,

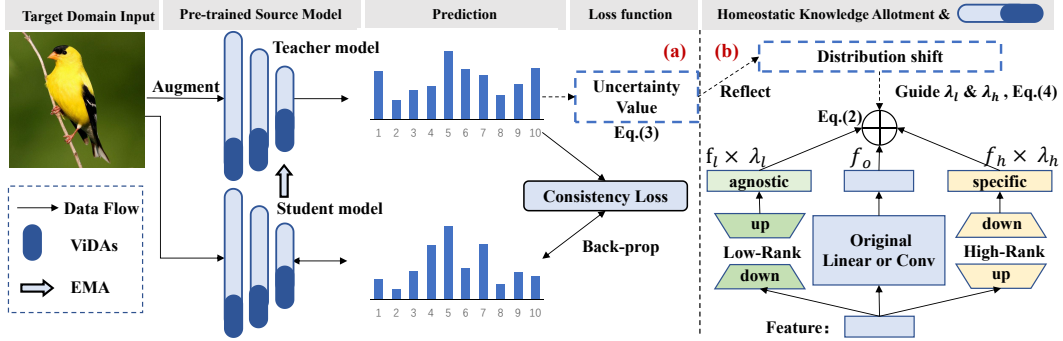


Figure 2: **The framework of Visual Domain Adapter (ViDA).** (a) We inject different domain-represented ViDAs into either linear or Conv layers of the pre-trained source model. To update the ViDAs, we construct a teacher-student framework and use a consistency loss (Eq. 5) as the optimization objective. The student model processes the original image, while the teacher model processes an augmented version of the same image. In addition to generating predictions, the teacher model calculates an uncertainty value (Eq. 3), reflecting the distribution shift of each sample in the target domain. (b) We illustrate the details of the Homeostatic Knowledge Allotment (HKA) strategy, which aims to dynamically fuse the knowledge from each ViDA with different rank prototypes.

$D_{T_1}, D_{T_2}, \dots, D_{T_n}$) are constantly changing over time. Our goal is to adapt the pre-trained model to target domains and maintain the perception ability of the model on the seen domain distribution.

Our approach proposes a novel Visual Domain Adapter (ViDA) that contains both high and low-dimensional prototypes. This design allows us to explicitly manage domain-specific and domain-agnostic knowledge, addressing the challenges of error accumulation and catastrophic forgetting in CTTA. To effectively adapt to the diverse distribution shifts, a Homeostatic Knowledge Allotment (HKA) strategy is introduced to dynamically fuse the knowledge from different ViDA with different domain representations. The overall framework is shown in Fig. 2.

3.1 Motivation

The Continual Test-Time Adaptation (CTTA) faces significant challenges, primarily due to error accumulation and catastrophic forgetting [59, 17]. Meanwhile, adapters with different dimension prototypes demonstrate remarkable effectiveness in addressing these challenges. This encourages us to take a step further and investigate the principles underlying the use of domain adapters in CTTA.

Adapter with low rank prototype. Our hypothesis regarding the effectiveness of adapters in mitigating catastrophic forgetting is that their low-rank prototype representation plays a crucial role. To explore this further, we conduct a t-SNE study [55] on the third transformer block to analyze the feature distributions across four target domains (ACDC). The results are depicted in Fig. 1 (b). Our analysis reveals that the low-rank adapter exhibits a relatively consistent distribution across the different target domains, suggesting that its low-rank prototype can effectively disregard the impact of dynamic distribution shifts and prioritize the extraction of domain-invariant knowledge.

We adopt the domain distance definition proposed by Ben-David [4, 3] and build upon previous domain transfer research [19] by employing the \mathcal{H} -divergence metric to further evaluate the domain representations of adapters across different target domains. \mathcal{H} -divergence between D_S and D_{T_i} can be calculated as $d_{\mathcal{H}}(D_S, D_{T_i}) = 2 \sup_{\mathcal{D} \sim \mathcal{H}} |\Pr_{x \sim D_S}[\mathcal{D}(x) = 1] - \Pr_{x \sim D_{T_i}}[\mathcal{D}(x) = 1]|$, where \mathcal{H} denotes hypothetical space and \mathcal{D} denotes discriminator. Similar to [19], calculating the \mathcal{H} -divergence directly is challenging. We adopt the *Jensen-Shannon (JS) divergence* between two adjacent domains as an approximation. To investigate the effectiveness of adapters in adapting to continual target domains, we compare the *JS* values obtained by using the source model alone, injecting low-rank adapter, and combining low-high adapters, as illustrated in Fig. 3 (a). Our results indicate that the feature representation generated by the low-rank adapter exhibits lower divergence compared to those of the original source model and closely resembles the values of low-high combination.

To provide clearer evidence for our assumption, we have developed an evaluation approach that directly reflects the extent of domain catastrophic forgetting. Shown in Table 1, after one round of CTTA on all target domains (ImageNet-C), we utilize the model and adapter from the last target

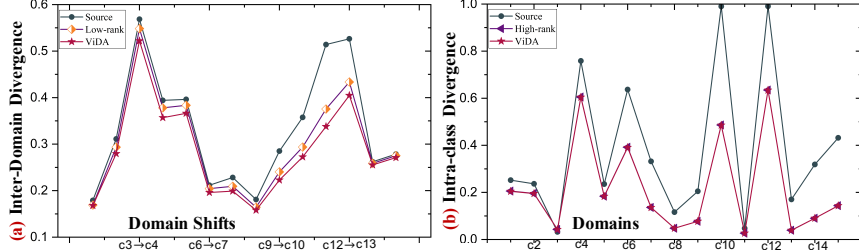


Figure 3: c1 to c15 represent the 15 corruption domains in CIFAR10C listed in sequential order. (a) Low-rank adapter based model effectively mitigates inter-domain divergence than the source model across all 14 domain shifts. (b) High-rank adapter based model significantly enhances the intra-class feature aggregation, yielding results that closely approximate those achieved by our ViDA method.

domain to directly test on previously seen target domains. As expected, the performance degradation is observed in only 2 out of 15 corruption types, and there is an overall improvement of 1.0% in the average classification error. These findings further support our assumptions and indicate that low-rank adapters are more effective in preserving continual domain-shared knowledge.

Adapter with high rank prototype. Regarding the domain representation of the adapter with a high-rank prototype, we propose that it is better suited to address error accumulation in the continual adaptation process. We verify this by visualizing the prototype distributions between different domains, as shown in Fig. 1 (b), and observe that there is a clear discrepancy between domains. And the distribution achieves a better aggregation in a single domain. This suggests that high-rank adapters primarily focus on extracting domain-specific knowledge in continual target domains. Inspired by intra-cluster dissimilarity proposed by k -means [42], we use normalized intra-class divergence to further verify the domain representations of high-rank adapters in CIFAR10C. As illustrated in Fig. 3 (b), the high-rank adapter is found to drive down divergence within almost all domains, indicating that it can better adapt to current domain distribution and extract domain-specific knowledge in continual target domains. To straightforwardly measure it, we quantitatively evaluate its performance. As shown in Table 6 *Ex2*, the classification error rate exhibits a sustained reduction (-4.6%) in the dynamic target domains with the use of a high-rank adapter. This finding supports our hypothesis that high-rank adapters can extract more reliable domain-specific knowledge.

3.2 Visual Domain Adapter

The above observation motivates us to introduce high-rank and low-rank Visual Domain Adapters (ViDAs) into the source pre-trained model, aiming to simultaneously adapt current domain distribution and maintain the continual domain-shared knowledge in CTTA.

The architecture. The design principle of injecting ViDAs into the pre-trained model is simple yet effective, which is illustrated in Figure .2 (b). As we can see there are three sub-branches, the linear (or Conv) layer in the middle branch is identical to the original network, while the right branch and left branch are bottleneck structures and separately indicate the high-rank ViDA and low-rank ViDA. Specifically, the right branch (high-rank) contains an up-projection layer with parameters $W_{up}^h \in R^{d \times d_h}$, a down-projection layer with parameters $W_{down}^h \in R^{d_h \times d}$, where d_h (i.e., $d_h = 128$) is the middle dimension of high-rank prototype and satisfies $d_h \geq d$. Note that, if the original feature dimension is higher than d_h , we will maintain the feature dimension within high-rank ViDA. Note that if the original feature dimension exceeds d_h , we will maintain the dimension within the high-rank ViDA. There is not any non-linear layer in the ViDA. And we utilize the linear layer as the projection layer when the original model is transformer architecture and adopt 1×1 Conv as the projection layer when the original model is a convolution network. In contrast, the left branch (low-rank) first injects a down-projection layer with parameters $W_{down}^l \in R^{d \times d_l}$, then place an up-projection layer with parameters $W_{up}^l \in R^{d_l \times d}$, where d_l (i.e., $d_l = 1$) stand for the middle dimension of the low-rank prototype ($d_l \ll d$). For an input feature f , the produced features of high-rank ViDA (f_h) and low-rank ViDA (f_l) are formulated as:

$$f_h = W_{down}^h \cdot (W_{up}^h \cdot f); \quad f_l = W_{up}^l \cdot (W_{down}^l \cdot f) \quad (1)$$

The two-branch bottleneck is connected to the output feature of the original network (f_o) through the residual connection via scale factors (λ_h and λ_l). The fusion knowledge (f_f) can be described as:

$$f_f = f_o + \lambda_h \times f_h + \lambda_l \times f_l \quad (2)$$

The domain knowledge scale factors (λ_h and λ_l) are adaptively obtained through the homeostatic knowledge allotment strategy, which is shown in Section 3.3.

Continual adapting. During the continual adaptation process, we freeze the parameters of the original model (middle branch) and update the high-rank ViDA and low-rank ViDA on the dynamic target domains with unsupervised loss. During inference, the different domain-represented ViDAs (linear relation) can be projected into the pre-trained model by re-parameterization [14], which ensures no extra parameter increase and maintain the plasticity of the original model.

3.3 Homeostatic Knowledge Allotment

Method motivation. In CTTA, the target domain data can only be accessed once and show different distribution shifts, which makes the efficiency of domain transfer crucial. Moreover, to tackle error accumulation and catastrophic forgetting effectively, it becomes necessary to extract different domain knowledge and handle them separately. This requires regularization of the knowledge fusion weight to ensure efficient capture of relevant domain-specific knowledge without sacrificing the retention of long-term domain-shared knowledge. **HKA design.** As depicted in Figure .2 (b), we draw inspiration from [45, 50, 18] and introduce an uncertainty value to quantify the degree of distribution shift for each sample. While the confidence score is a common measure to assess prediction reliability, it tends to fluctuate irregularly and becomes unreliable in scenarios characterized by distribution shifts. To address this limitation, we employ the MC Dropout technique [16] on linear layers, enabling multiple forward propagations to obtain m sets of probabilities for each sample. Subsequently, we calculate the uncertainty value $\mathcal{U}(x)$ for a given input x , which are formulated as:

$$\mathcal{U}(x) = \left(\frac{1}{m} \sum_{i=1}^m \|p_i(y|x) - \mu\|^2 \right)^{\frac{1}{2}} \quad (3)$$

Where $p_i(y|x)$ is the predicted probability of the input x in the i^{th} forward propagation and μ is the average value of m times prediction. To dynamically adjust the scale factors (λ_h and λ_l) based on the uncertainty score, the formulation is as follows:

$$\begin{cases} \lambda_h = 1 + \mathcal{U}(x) & \lambda_l = 1 - \mathcal{U}(x), & \mathcal{U}(x) \geq \Theta \\ \lambda_h = 1 - \mathcal{U}(x) & \lambda_l = 1 + \mathcal{U}(x), & \mathcal{U}(x) < \Theta \end{cases} \quad (4)$$

The threshold value of uncertainty is denoted as Θ , where $\Theta = 0.2$. To realize the homeostasis of different domain knowledge, when facing the sample with a large uncertainty value, we adaptively increase the fusion weight of domain-specific knowledge (λ_h). Conversely, if the input has a low uncertainty value, the fusion weight of domain-agnostic knowledge (λ_l) will be increased. By employing the HKA strategy, our approach ensures that the adaptation process effectively captures relevant domain-specific knowledge while retaining long-term domain-shared knowledge.

3.4 Optimization Objective

Following previous CTTA work [59, 17], we leverage the teacher model \mathcal{T} to generate the pseudo labels \tilde{y} for updating ViDAs. And we adopt consistency loss L_{ce} as the optimization objective.

$$\mathcal{L}_{ce}(x) = -\frac{1}{C} \sum_c \tilde{y}(c) \log \hat{y}(c) \quad (5)$$

Where \hat{y} is the output of our student model \mathcal{S} , C means the number of categories. Same as previous works[59, 17], we load the source pre-trained parameters to initialize the weight of both models and adopt the exponential moving average (EMA) to update the teacher model with ViDAs.

$$\mathcal{T}^t = \alpha \mathcal{T}^{t-1} + (1 - \alpha) \mathcal{S}^t \quad (6)$$

Where t is the time step. And we set $\alpha = 0.999$ [54], which is the updating weight of EMA.

4 Experiment

In Section 4.2 and 4.3, we compare our method with other SOTA methods on classification and segmentation of CTTA. In Section 4.4, we employ the foundation model [33, 44] as the backbone

and evaluate the efficacy of our method. In Section 4.5, we further evaluate the domain generalization ability of the proposed method. Comprehensive ablation studies are conducted in Section 4.6. More quantitative comparisons and qualitative analyses are shown in the supplementary materials.

4.1 Task settings and Datasets

Dataset. We evaluate our method on three classification CTTA benchmarks, including CIFAR10-to-CIFAR10C(standard), CIFAR100-to-CIFAR100C [34] and ImageNet-to-ImageNet-C [25]. For segmentation CTTA [59, 61], we evaluate our method on Cityscapes-to-ACDC, where the Cityscapes dataset [12] serves as the source domain, and the ACDC dataset [51] represents the target domains.

Baselines. We compare the proposed method against two types of CTTA approaches, including (1)Modal-based: source model [15, 60], Pseudo-label [37], Tent-continual [58], CoTTA [59], and SATA [8]. (2) Prompt-based: visual domain prompt [17].

CTTA Task setting. Following [59, 17], in classification CTTA tasks, we sequentially adapt the pre-trained source model to the fifteen target domains with the largest corruption severity (level 5). The online prediction results were evaluated immediately after encountering the input data. Regarding segmentation CTTA [59, 61], the source model [60] is an off-the-shelf pre-trained on the Cityscapes dataset [12]. As for the continual target domains, we utilize the ACDC dataset [51], which consists of images collected in four unseen visual conditions: Fog, Night, Rain, and Snow. To simulate continual environmental changes in real-life scenarios, we cyclically repeat the same sequence of target domains (Fog→Night→Rain→Snow) multiple times.

Implementation Details. In our CTTA experiments, we follow the implementation details specified in previous works [59, 61] to ensure consistency and comparability. we adopt ViT-base [15] and ResNet [23] as the backbone in classification CTTA. In the case of ViT-base, we resize the input images to 224x224, while maintaining the original image resolution for other backbones. For segmentation CTTA, we adopt the pre-trained Segformer-B5 model [60] as the source model. We down-sample the input size from 1920x1080 to 960x540 for target domain data [59]. The optimizer is performed using Adam [32] with $(\beta_1, \beta_2) = (0.9, 0.999)$. We set the learning rates to specific values for each backbone, such as 1e-5 for ViT and 3e-4 for Segformer. To initialize our visual domain adapters, we train the model with adapters for one epoch on the source domain. We apply a range of image resolution scale factors [0.5, 0.75, 1.0, 1.25, 1.5, 1.75, 2.0] for the augmentation method and construct the teacher model inputs [59]. All experiments are conducted on NVIDIA A100 GPUs.

4.2 The Effectiveness on Classification CTTA

Table 1: Classification error rate(%) for ImageNet-to-ImageNet-C online CTTA task. Gain(%) represents the percentage of improvement in model accuracy compared with the source method.

Backbone	Method	REF	Gaussian	shot	impulse	defocus	glass	motion	zoom	snow	frost	fog	brightness	contrast	elastic_trans	pixelate	jpeg	Mean↓	Gain
ResNet50	Source [22]	CVPR2016	97.8	97.1	98.2	81.7	89.8	85.2	78	83.5	77.1	75.9	41.3	94.5	82.5	79.3	68.6	82	0.0
	CoTTA [59]	CVPR2022	52.9	51.6	51.4	68.3	78.1	57.1	62.0	48.2	52.7	55.3	25.9	90.0	56.4	36.4	35.2	62.7	+19.3
	VDP [17]	AAAI2023	-	-	-	-	-	-	-	-	-	-	-	-	-	-	-	51.5	+30.5
	SATA [8]	2023.4.20	74.1	72.9	71.6	75.7	74.1	64.2	55.5	55.6	62.9	46.6	36.1	69.9	50.6	44.3	48.5	60.1	+21.9
ViT-base	Source	ICLR2021	53.0	51.8	52.1	68.5	78.8	58.5	63.3	49.9	54.2	57.7	26.4	91.4	57.5	38.0	36.2	55.8	0.0
	Pseudo [37]	ICML2013	45.2	40.4	41.6	51.3	53.9	45.6	47.7	40.4	45.7	93.8	98.5	99.9	99.9	98.9	99.6	61.2	-5.4
	Tent [58]	ICLR2021	52.2	48.9	49.2	65.8	73	54.5	58.4	44.0	47.7	50.3	23.9	72.8	55.7	34.4	33.9	51.0	+4.8
	CoTTA [59]	CVPR2022	52.9	51.6	51.4	68.3	78.1	57.1	62.0	48.2	52.7	55.3	25.9	90.0	56.4	36.4	35.2	54.8	+3.6
	VDP [17]	AAAI2023	52.7	51.6	50.1	58.1	70.2	56.1	58.1	42.1	46.1	45.8	23.6	70.4	54.9	34.5	36.1	50.0	+5.8
	Ours	Proposed	47.7	42.5	42.9	52.2	56.9	45.5	48.9	38.9	42.7	40.7	24.3	52.8	49.1	33.5	33.1	43.4	+12.4
Directly test after adaptation																		Mean↓	Gain
ViT-base	Ours	Proposed	46.2	44.4	45.8	48.9	52.1	45.0	48.6	37.5	41.9	39.5	23.9	49.0	49.0	32.1	32.6	42.4	+13.4

ImageNet-to-ImageNet-C. Given the source model pre-trained on ImageNet, we conduct CTTA on ImageNet-C, which consists of fifteen corruption types that occur sequentially during the test time. Table .1 demonstrates that the majority of methods employing the ViT backbone achieve lower classification errors compared to those using the ResNet50 backbone. For ViT-base, the average classification error is up to 55.8% when we directly test the source model on target domains. In contrast, our method can outperform all previous methods, achieving a 12.4% and 6.6% improvement

Table 2: Average error rate (%) for the standard CIFAR10-to-CIAFAR10C and CIFAR100-to-CIAFAR100C CTTA task. All results are evaluated on the ViT-base, which is fully pre-trained on the source domain dataset.

Target	Method	Source	Tent	CoTTA	VDP	Ours
Cifar10C	Mean↓	28.2	25.5	24.6	24.1	20.7
	Gain↑	0.0	+2.7	+3.6	+4.1	+7.5
Cifar100C	Mean↓	35.4	33.2	34.8	35.0	27.3
	Gain↑	0.0	+2.2	+0.7	+0.4	+8.1

over the source model and previous SOTA method, respectively. Moreover, our method showcases remarkable performance across the majority of corruption types, highlighting its effective mitigation of error accumulation and its capability for continual adaptation. After completing the entire CTTA process, we evaluate the performance of our method on the seen target domains. As shown in Table 1, the performance degradation is observed in only 2 out of 15 corruption types. Additionally, we achieve an overall improvement of 1.0% in the average classification error. These findings demonstrate that our method successfully preserves continual domain-shared knowledge and avoids catastrophic forgetting during CTTA. In conclusion, our homeostatic ViDAs can extract the different domain knowledge and avoid CTTA main challenges simultaneously.

To further validate the effectiveness of our method, we conduct experiments on CIFAR10-to-CIFAR10C and CIFAR100-to-CIFAR100C. As illustrated in Table .2, in CIFAR10C, our approach achieved a 3.4% improvement compared to the previous SOTA model. We extend our evaluation to CIFAR100C, which comprises a larger number of categories in each domain. Our approach surpasses all previous methods, which show the same trend as the above CTTA experiments. Therefore, the results prove that our method mitigates the challenges posed by continual distribution shifts, regardless of the number of categories present in each domain.

4.3 The Effectiveness on Segmentation CTTA

Table 4: **Performance comparison for Cityscape-to-ACDC CTTA.** We sequentially repeat the same sequence of target domains three times. Mean is the average score of mIoU.

Time Round	Method	REF	t →															Mean↑	Gain	
			1					2					3							
			Fog	Night	Rain	Snow	Mean↑	Fog	Night	Rain	Snow	Mean↑	Fog	Night	Rain	Snow	Mean↑			
Source [60]	NIPS2021		69.1	40.3	59.7	57.8	56.7	69.1	40.3	59.7	57.8	56.7	69.1	40.3	59.7	57.8	56.7	56.7	56.7	/
TENT [57]	ICLR2021		69.0	40.2	60.1	57.3	56.7	68.3	39.0	60.1	56.3	55.9	67.5	37.8	59.6	55.0	55.0	55.7	55.7	-1.0
CoTTA [59]	CVPR2022		70.9	41.2	62.4	59.7	58.6	70.9	41.1	62.6	59.7	58.6	70.9	41.0	62.7	59.7	58.6	58.6	58.6	+1.9
DePT [21]	ICLR2023		71.0	40.8	58.2	56.8	56.5	68.2	40.0	55.4	53.7	54.3	66.4	38.0	47.3	47.2	49.7	53.4	53.4	-3.3
VDP [17]	AAAI2023		70.5	41.1	62.1	59.5	58.3	70.4	41.1	62.2	59.4	58.2	70.4	41.0	62.2	59.4	58.2	58.2	58.2	+1.5
Ours	Proposed		71.6	43.2	66.0	63.4	61.1	73.2	44.5	67.0	63.9	62.2	73.2	44.6	67.2	64.2	62.3	61.9	61.9	+5.2

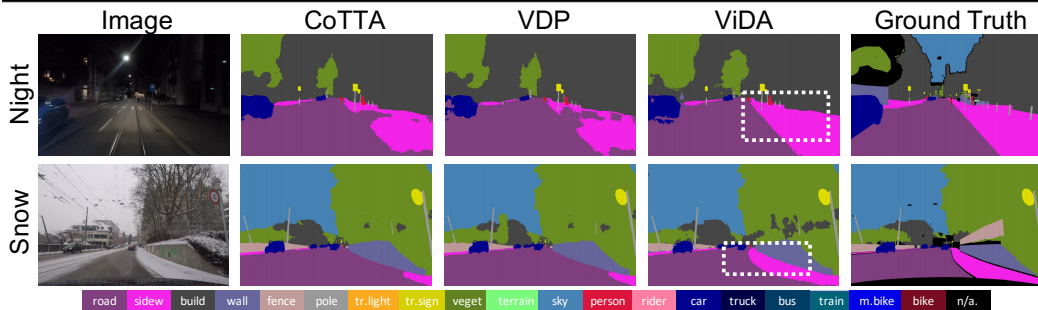


Figure 4: Qualitative comparison of our method with previous SOTA methods on the ACDC dataset. Our method could better segment different pixel-wise classes such as shown in the white box.

Cityscapes-to-ACDC. To demonstrate the effectiveness of our method in the semantic segmentation CTTA task, we conducted evaluations on four target domains from the ACDC dataset periodically during test time. As presented in Table 4, we observed a gradual decrease in the mIoUs of TENT and DePT over time, indicating the occurrence of catastrophic forgetting. In contrast, our method has a continual improvement of average mIoU (61.1→62.2→62.3) when the same sequence of target domains is repeated. Significantly, the proposed method surpasses the previous state-of-the-art

Table 5: The domain generalization comparisons on ImageNet-C. Results are evaluated on ViT-base. Mean and Gain(%) represent the performance on unseen target domains.

Method	Directly test on unseen domains					Unseen
	bri.	contrast	elastic	pixelate	jpeg	Mean↓
Source	26.4	91.4	57.5	38.0	36.2	49.9
Tent	25.8	91.9	57.0	37.2	35.7	49.5
CoTTA	25.3	88.1	55.7	36.4	34.6	48.0
Ours	24.6	68.2	49.8	34.7	34.1	42.3

Table 6: Average error rate (%) for the ImageNet-to-ImageNet-C. Results are evaluated on the ViT. $ViDA_h$ and $ViDA_l$ represent the ViDAs with high-rank and low-rank prototypes.

	$ViDA_h$	$ViDA_l$	HKA	Mean↓
Ex_1	-	-	-	55.8
Ex_2	✓	-	-	51.2
Ex_3	-	✓	-	50.7
Ex_4	✓	✓	-	45.6
Ex_5	✓	✓	✓	43.4

CTTA method [59] by achieving a 3.3% increase in mIoU. This notable improvement showcases our method’s ability to adapt continuously to different target domains in the pixel-level task. In Fig .4, our method correctly distinguish the sidewalk from the road, avoiding mis-classification.

4.4 Continual Adapting for Foundation Models

Foundation models [5] are trained on large-scale datasets, endowing them with powerful generalization capabilities and the ability to capture representations of common features. However, performing full fine-tuning on the foundation model is time-consuming and economically impractical. Hence, our adaptation method proves valuable by enhancing the continual transfer performance of foundation models. As indicated in Table. 3, we introduce foundation models as the pre-trained model and adapt them to continual target domains (CIFAR10C). Our approach achieved a performance improvement of 4.8% on the representative image-level foundation model DINOv2 [44] and 5.2% on pixel-level foundation model SAM [33]. Our method consistently and reliably improves the performance of the foundation model on the unseen continual target domains. Note that, we only use the pre-trained encoder of SAM and add a classification head, which is fine-tuned on the source domain. During the inference phase, the ViDAs with a linear relationship can be projected onto the pre-trained foundation model through re-parameterization. This process empowers the foundation model with the learned different domain representations and maintains the model plasticity.

4.5 Domain Generalization on Unseen Continual Domains

To investigate the domain generalization (DG) ability of our method, we follow the leave-one-domain-out rule [65, 39] to leverage 10/15 domains of ImageNet-C as source domains for model training while the rest (5/15 domains) are treated as target domains without any form of adaptation. Specifically, we first use our proposed method to continually adapt the pre-trained model to 10/15 domains of ImageNet-C without any supervision. Then we directly test on the 5/15 unseen domains. Surprisingly, our method reduces 7.6% on the average error on unseen domains (Table 5), which has a significant improvement over other methods. The promising results demonstrate that our method possesses DG ability by effectively extracting domain-agnostic knowledge. This finding provides a new perspective on enhancing DG performance. More DG experiments are provided in the supplementary materials.

4.6 Ablation study

Effectiveness of each component. We conduct the ablation study on ImageNet-to-ImageNet-C CTTA scenario and evaluate the contribution of each component in our method, including high-rank ViDA ($ViDA_h$), low-rank ViDA ($ViDA_l$), and Homeostatic Knowledge Allotment (HKA) strategy. As shown in Table .6, Ex_1 represents the performance of the source pre-trained model (only 55.8%). In Ex_2 , by introducing the high-rank ViDA, the average error decrease 4.6%, demonstrating that the high-rank prototype can extract more domain-specific knowledge to adapt in target domains. As illustrated in Ex_3 , low-rank ViDA gains 5.1% improvement compared to Ex_1 . The result proves that the domain-share knowledge extracted from low-rank prototypes can also improve the classification ability on continual target domains. Ex_4 has a remarkable improvement of 10.2% overall, demonstrating that the two types of ViDA can compensate for each other in the continual adaptation process. Ex_5 achieves 12.4% improvement in total, showcasing the effectiveness of the HKA strategy in maximizing the CTTA potential of both types of ViDA.

5 Conclusion and Limitations

In this paper, we propose a homeostatic Visual Domain Adapter (ViDA) to address error accumulation and catastrophic forgetting problems in Continual Test-Time Adaptation (CTTA) tasks. And we investigate that the low-rank ViDA can disregard the impact of dynamic distribution shifts and prioritize the extraction of domain-invariant knowledge, and the high-rank ViDA can extract more reliable domain-specific knowledge. Meanwhile, we further propose a Homeostatic Knowledge Allotment (HKA) strategy to dynamically fuse the knowledge from each ViDA with different rank prototypes. For limitations, the injected ViDAs and teacher-student scheme brings extra parameters and computational costs during the continual adaptation process. However, the ViDAs can be projected into the original model by re-parameterization and the teacher-student framework only preserve one model during inference.

Acknowledgement. We thank Xiaoqi Li for the insightful discussions and for helping with writing.

References

- [1] Eduardo Arnold, Omar Y Al-Jarrah, Mehrdad Dianati, Saber Fallah, David Oxtoby, and Alex Mouzakitis. A survey on 3d object detection methods for autonomous driving applications. *IEEE Transactions on Intelligent Transportation Systems*, 20(10):3782–3795, 2019.
- [2] Hyojin Bahng, Ali Jahanian, Swami Sankaranarayanan, and Phillip Isola. Exploring visual prompts for adapting large-scale models. 2022.
- [3] Shai Ben-David, John Blitzer, Koby Crammer, Alex Kulesza, Fernando Pereira, and Jennifer Wortman Vaughan. A theory of learning from different domains. *Machine learning*, 79(1):151–175, 2010.
- [4] Shai Ben-David, John Blitzer, Koby Crammer, and Fernando Pereira. Analysis of representations for domain adaptation. *Advances in neural information processing systems*, 19, 2006.
- [5] Rishi Bommasani, Drew A Hudson, Ehsan Adeli, Russ Altman, Simran Arora, Sydney von Arx, Michael S Bernstein, Jeannette Bohg, Antoine Bosselut, Emma Brunskill, et al. On the opportunities and risks of foundation models. *arXiv preprint arXiv:2108.07258*, 2021.
- [6] Malik Boudiaf, Tom Denton, Bart van Merriënboer, Vincent Dumoulin, and Eleni Triantafillou. In search for a generalizable method for source free domain adaptation. 2023.
- [7] Malik Boudiaf, Romain Mueller, Ismail Ben Ayed, and Luca Bertinetto. Parameter-free online test-time adaptation. *ArXiv*, abs/2201.05718, 2022.
- [8] Goirik Chakrabarty, Manogna Sreenivas, and Soma Biswas. Sata: Source anchoring and target alignment network for continual test time adaptation. *arXiv preprint arXiv:2304.10113*, 2023.
- [9] Dian Chen, Dequan Wang, Trevor Darrell, and Sayna Ebrahimi. Contrastive test-time adaptation. *ArXiv*, abs/2204.10377, 2022.
- [10] Liang-Chieh Chen, George Papandreou, Iasonas Kokkinos, Kevin Murphy, and Alan L Yuille. Deeplab: Semantic image segmentation with deep convolutional nets, atrous convolution, and fully connected crfs. *IEEE transactions on pattern analysis and machine intelligence*, 40(4):834–848, 2017.
- [11] Shoufa Chen, GE Chongjian, Zhan Tong, Jiangliu Wang, Yibing Song, Jue Wang, and Ping Luo. Adaptformer: Adapting vision transformers for scalable visual recognition. In *Advances in Neural Information Processing Systems*.
- [12] Marius Cordts, Mohamed Omran, Sebastian Ramos, Timo Rehfeld, Markus Enzweiler, Rodrigo Benenson, Uwe Franke, Stefan Roth, and Bernt Schiele. The cityscapes dataset for semantic urban scene understanding. In *Proceedings of the IEEE conference on computer vision and pattern recognition*, pages 3213–3223, 2016.
- [13] Ning Ding, Yujia Qin, Guang Yang, Fuchao Wei, Zonghan Yang, Yusheng Su, Shengding Hu, Yulin Chen, Chi-Min Chan, Weize Chen, et al. Parameter-efficient fine-tuning of large-scale pre-trained language models. *Nature Machine Intelligence*, pages 1–16, 2023.

- [14] Xiaohan Ding, Xiangyu Zhang, Ningning Ma, Jungong Han, Guiguang Ding, and Jian Sun. Reprvgg: Making vgg-style convnets great again. In *Proceedings of the IEEE/CVF conference on computer vision and pattern recognition*, pages 13733–13742, 2021.
- [15] Alexey Dosovitskiy, Lucas Beyer, Alexander Kolesnikov, Dirk Weissenborn, Xiaohua Zhai, Thomas Unterthiner, Mostafa Dehghani, Matthias Minderer, Georg Heigold, Sylvain Gelly, et al. An image is worth 16x16 words: Transformers for image recognition at scale. *arXiv preprint arXiv:2010.11929*, 2020.
- [16] Yarin Gal and Zoubin Ghahramani. Dropout as a bayesian approximation: Representing model uncertainty in deep learning. In *international conference on machine learning*, pages 1050–1059. PMLR, 2016.
- [17] Yulu Gan, Xianzheng Ma, Yihang Lou, Yan Bai, Renrui Zhang, Nian Shi, and Lin Luo. Decorate the newcomers: Visual domain prompt for continual test time adaptation. *arXiv preprint arXiv:2212.04145*, 2022.
- [18] Yulu Gan, Mingjie Pan, Rongyu Zhang, Zijian Ling, Lingran Zhao, Jiaming Liu, and Shanghang Zhang. Cloud-device collaborative adaptation to continual changing environments in the real-world. *arXiv preprint arXiv:2212.00972*, 2022.
- [19] Yaroslav Ganin, Evgeniya Ustinova, Hana Ajakan, Pascal Germain, Hugo Larochelle, François Laviolette, Mario Marchand, and Victor Lempitsky. Domain-adversarial training of neural networks. *The journal of machine learning research*, 17(1):2096–2030, 2016.
- [20] Tianyu Gao, Adam Fisch, and Danqi Chen. Making pre-trained language models better few-shot learners. In *Joint Conference of the 59th Annual Meeting of the Association for Computational Linguistics and the 11th International Joint Conference on Natural Language Processing, ACL-IJCNLP 2021*, pages 3816–3830. Association for Computational Linguistics (ACL), 2021.
- [21] Yunhe Gao, Xingjian Shi, Yi Zhu, Hao Wang, Zhiqiang Tang, Xiong Zhou, Mu Li, and Dimitris N Metaxas. Visual prompt tuning for test-time domain adaptation. *arXiv preprint arXiv:2210.04831*, 2022.
- [22] Kaiming He, Xiangyu Zhang, Shaoqing Ren, and Jian Sun. Delving deep into rectifiers: Surpassing human-level performance on imagenet classification. *international conference on computer vision*, 2015.
- [23] Kaiming He, Xiangyu Zhang, Shaoqing Ren, and Jian Sun. Deep residual learning for image recognition. In *Proceedings of the IEEE conference on computer vision and pattern recognition*, pages 770–778, 2016.
- [24] Ruidan He, Linlin Liu, Hai Ye, Qingyu Tan, Bosheng Ding, Liying Cheng, Jia-Wei Low, Lidong Bing, and Luo Si. On the effectiveness of adapter-based tuning for pretrained language model adaptation. *arXiv preprint arXiv:2106.03164*, 2021.
- [25] Dan Hendrycks and Thomas Dietterich. Benchmarking neural network robustness to common corruptions and perturbations. *arXiv preprint arXiv:1903.12261*, 2019.
- [26] Neil Houlsby, Andrei Giurgiu, Stanislaw Jastrzebski, Bruna Morrone, Quentin De Laroussilhe, Andrea Gesmundo, Mona Attariyan, and Sylvain Gelly. Parameter-efficient transfer learning for nlp. In *International Conference on Machine Learning*, pages 2790–2799. PMLR, 2019.
- [27] Edward J Hu, Yelong Shen, Phillip Wallis, Zeyuan Allen-Zhu, Yuanzhi Li, Shean Wang, Lu Wang, and Weizhu Chen. Lora: Low-rank adaptation of large language models. *arXiv preprint arXiv:2106.09685*, 2021.
- [28] Shengding Hu, Ning Ding, Huadong Wang, Zhiyuan Liu, Jingang Wang, Juanzi Li, Wei Wu, and Maosong Sun. Knowledgeable prompt-tuning: Incorporating knowledge into prompt verbalizer for text classification. In *Proceedings of the 60th Annual Meeting of the Association for Computational Linguistics (Volume 1: Long Papers)*, pages 2225–2240, 2022.
- [29] Yu Huang and Yue Chen. Autonomous driving with deep learning: A survey of state-of-art technologies. *arXiv preprint arXiv:2006.06091*, 2020.

- [30] Menglin Jia, Luming Tang, Bor-Chun Chen, Claire Cardie, Serge Belongie, Bharath Hariharan, and Ser-Nam Lim. Visual prompt tuning. 2022.
- [31] Rabeeh Karimi Mahabadi, James Henderson, and Sebastian Ruder. Compacter: Efficient low-rank hypercomplex adapter layers. *Advances in Neural Information Processing Systems*, 34:1022–1035, 2021.
- [32] Diederik P Kingma and Jimmy Ba. Adam: A method for stochastic optimization. *arXiv preprint arXiv:1412.6980*, 2014.
- [33] Alexander Kirillov, Eric Mintun, Nikhila Ravi, Hanzi Mao, Chloe Rolland, Laura Gustafson, Tete Xiao, Spencer Whitehead, Alexander C Berg, Wan-Yen Lo, et al. Segment anything. *arXiv preprint arXiv:2304.02643*, 2023.
- [34] Alex Krizhevsky, Geoffrey Hinton, et al. Learning multiple layers of features from tiny images. 2009.
- [35] Jogendra Nath Kundu, Naveen Venkat, Rahul M, and R. Venkatesh Babu. Universal source-free domain adaptation. 2020.
- [36] Qicheng Lao, Xiang Jiang, and Mohammad Havaei. Hypothesis disparity regularized mutual information maximization, 2020.
- [37] Dong-Hyun Lee. Pseudo-label : The simple and efficient semi-supervised learning method for deep neural networks. 2013.
- [38] Brian Lester, Rami Al-Rfou, and Noah Constant. The power of scale for parameter-efficient prompt tuning. *arXiv preprint arXiv:2104.08691*, 2021.
- [39] Da Li, Yongxin Yang, Yi-Zhe Song, and Timothy M Hospedales. Deeper, broader and artier domain generalization. In *Proceedings of the IEEE international conference on computer vision*, pages 5542–5550, 2017.
- [40] Jian Liang, Ran He, and Tieniu Tan. A comprehensive survey on test-time adaptation under distribution shifts. *arXiv preprint arXiv:2303.15361*, 2023.
- [41] Jian Liang, D. Hu, and Jiashi Feng. Do we really need to access the source data? source hypothesis transfer for unsupervised domain adaptation. In *ICML*, 2020.
- [42] J MacQueen. Classification and analysis of multivariate observations. In *5th Berkeley Symp. Math. Statist. Probability*, pages 281–297. University of California Los Angeles LA USA, 1967.
- [43] Chaithanya Kumar Mummadi, Robin Huttmacher, Kilian Rambach, Evgeny Levinkov, Thomas Brox, and Jan Hendrik Metzen. Test-time adaptation to distribution shift by confidence maximization and input transformation. *arXiv preprint arXiv:2106.14999*, 2021.
- [44] Maxime Oquab, Timothée Darcet, Théo Moutakanni, Huy Vo, Marc Szafraniec, Vasil Khalidov, Pierre Fernandez, Daniel Haziza, Francisco Massa, Alaaeldin El-Nouby, et al. Dinov2: Learning robust visual features without supervision. *arXiv preprint arXiv:2304.07193*, 2023.
- [45] Yaniv Ovadia, Emily Fertig, Jie Ren, Zachary Nado, David Sculley, Sebastian Nowozin, Joshua Dillon, Balaji Lakshminarayanan, and Jasper Snoek. Can you trust your model’s uncertainty? evaluating predictive uncertainty under dataset shift. *Advances in neural information processing systems*, 32, 2019.
- [46] Yujia Qin, Xiaozhi Wang, Yusheng Su, Yankai Lin, Ning Ding, Zhiyuan Liu, Juanzi Li, Lei Hou, Peng Li, Maosong Sun, et al. Exploring low-dimensional intrinsic task subspace via prompt tuning. *arXiv preprint arXiv:2110.07867*, 2021.
- [47] Sylvestre-Alvise Rebuffi, Hakan Bilen, and Andrea Vedaldi. Learning multiple visual domains with residual adapters. *Advances in neural information processing systems*, 30, 2017.
- [48] Sylvestre-Alvise Rebuffi, Hakan Bilen, and Andrea Vedaldi. Efficient parametrization of multi-domain deep neural networks. In *Proceedings of the IEEE Conference on Computer Vision and Pattern Recognition*, pages 8119–8127, 2018.

- [49] Shaoqing Ren, Kaiming He, Ross Girshick, and Jian Sun. Faster r-cnn: Towards real-time object detection with region proposal networks. *Advances in neural information processing systems*, 28, 2015.
- [50] Subhankar Roy, Martin Trapp, Andrea Pilzer, Juho Kannala, Nicu Sebe, Elisa Ricci, and Arno Solin. Uncertainty-guided source-free domain adaptation. In *Computer Vision–ECCV 2022: 17th European Conference, Tel Aviv, Israel, October 23–27, 2022, Proceedings, Part XXV*, pages 537–555. Springer, 2022.
- [51] Christos Sakaridis, Dengxin Dai, and Luc Van Gool. Acdc: The adverse conditions dataset with correspondences for semantic driving scene understanding. In *Proceedings of the IEEE/CVF International Conference on Computer Vision*, pages 10765–10775, 2021.
- [52] Steffen Schneider, Evgenia Rusak, Luisa Eck, Oliver Bringmann, Wieland Brendel, and Matthias Bethge. Improving robustness against common corruptions by covariate shift adaptation. *ArXiv*, abs/2006.16971, 2020.
- [53] Yi-Lin Sung, Jaemin Cho, and Mohit Bansal. V1-adapter: Parameter-efficient transfer learning for vision-and-language tasks. In *Proceedings of the IEEE/CVF Conference on Computer Vision and Pattern Recognition*, pages 5227–5237, 2022.
- [54] Antti Tarvainen and Harri Valpola. Mean teachers are better role models: Weight-averaged consistency targets improve semi-supervised deep learning results. *Learning*, 2017.
- [55] Laurens Van der Maaten and Geoffrey Hinton. Visualizing data using t-sne. *Journal of machine learning research*, 9(11), 2008.
- [56] Tu Vu, Brian Lester, Noah Constant, Rami Al-Rfou, and Daniel Cer. Spot: Better frozen model adaptation through soft prompt transfer. In *Proceedings of the 60th Annual Meeting of the Association for Computational Linguistics (Volume 1: Long Papers)*, pages 5039–5059, 2022.
- [57] Dequan Wang, Evan Shelhamer, Shaoteng Liu, Bruno Olshausen, and Trevor Darrell. Tent: Fully test-time adaptation by entropy minimization. *arXiv preprint arXiv:2006.10726*, 2020.
- [58] Dequan Wang, Evan Shelhamer, Shaoteng Liu, Bruno A. Olshausen, and Trevor Darrell. Tent: Fully test-time adaptation by entropy minimization. In *ICLR*, 2021.
- [59] Qin Wang, Olga Fink, Luc Van Gool, and Dengxin Dai. Continual test-time domain adaptation. *ArXiv*, abs/2203.13591, 2022.
- [60] Enze Xie, Wenhai Wang, Zhiding Yu, Anima Anandkumar, Jose M Alvarez, and Ping Luo. Segformer: Simple and efficient design for semantic segmentation with transformers. *Advances in Neural Information Processing Systems*, 34:12077–12090, 2021.
- [61] Senqiao Yang, Jiarui Wu, Jiaming Liu, Xiaoqi Li, Qizhe Zhang, Mingjie Pan, and Shanghang Zhang. Exploring sparse visual prompt for cross-domain semantic segmentation. *arXiv preprint arXiv:2303.09792*, 2023.
- [62] Shiqi Yang, Yaxing Wang, Joost van de Weijer, Luis Herranz, and Shangling Jui. Generalized source-free domain adaptation. *international conference on computer vision*, 2021.
- [63] Sergey Zagoruyko and Nikos Komodakis. Wide residual networks. *british machine vision conference*, 2016.
- [64] Elad Ben Zaken, Shauli Ravfogel, and Yoav Goldberg. Bitfit: Simple parameter-efficient fine-tuning for transformer-based masked language-models. *arXiv preprint arXiv:2106.10199*, 2021.
- [65] Kaiyang Zhou, Ziwei Liu, Yu Qiao, Tao Xiang, and Chen Change Loy. Domain generalization in vision: A survey. *arXiv preprint arXiv:2103.02503*, 2021.
- [66] Xizhou Zhu, Weijie Su, Lewei Lu, Bin Li, Xiaogang Wang, and Jifeng Dai. Deformable detr: Deformable transformers for end-to-end object detection. *arXiv preprint arXiv:2010.04159*, 2020.

A Appendix

The supplementary materials presented in this paper offer a comprehensive quantitative and qualitative analysis of the proposed method. In Section B, we provide additional implementation details regarding the evidence of motivation. And we also present an extra continual adaptation experiment for Foundation Models in Section C.1, which is conducted on ImageNet-to-ImageNet-C. To evaluate the domain generalization ability of our method, we conducted additional experiments directly testing on a different number of unseen domains in Section C.2. Ablation study on prototype dimension are described in Section C.3. Furthermore, Section C.4 presents additional CTTA classification experiments utilizing the convolutional backbone. We offer an additional qualitative analysis in Section D. In Section E, we present a more detailed discussion of related work. Moreover, we extend the classification results of our submission to include a fine-grained performance, which examines the error across fifteen corruption types. The checklist is presented in the final section of this report.

B Supplementary Details for Motivation

The study of Continual Test-Time Adaptation (CTTA) poses significant challenges, particularly in addressing error accumulation and catastrophic forgetting [59, 17]. Notably, the use of adapters with prototypes of varying dimensions has demonstrated promising results in mitigating these challenges in our submission. In this section, we aim to provide comprehensive implementation details regarding the evidence supporting our motivation. Furthermore, we delve deeper the underlying principles behind the effective utilization of domain adapters.

Distribution Qualitative Analysis We employ t-distributed stochastic neighbor embedding (t-SNE) [55] to visualize the distribution of adapters across four continual target domains. This visualization is specifically performed on the Cityscapes-to-ACDC experiment, which represents a scenario with continually changing environments in the real world. To conduct the t-SNE analysis, we analyze the output of the third transformer block in the Segformer-B5 model [60]. The objective is to qualitatively compare the feature distributions of adapters with different dimension prototypes. Furthermore, our findings reveal that the qualitative results obtained from different layers of the Segformer-B5 model exhibit similar distribution representations. Illustrated in Figure 1(b) of our submission, there is a noticeable distribution gap due to the significant domain shift between the night domain and other domains. Interestingly, the low-rank Visual Domain Adapter (ViDA) effectively reduces the distribution distance across different target domains. On the other hand, the high-rank ViDA exhibits notable distribution discrepancies among the various target domains, indicating its focus on extracting domain-specific knowledge.

Distribution Distance To provide clearer evidence for our assumption, we directly calculate the distribution distance to represent different domain representation of adapters. We adopt the domain distance definition proposed by Ben-David [4, 3] and build upon previous domain transfer research [19] by employing the \mathcal{H} -divergence metric to further evaluate the domain representations of adapters across different target domains. \mathcal{H} -divergence between D_S and D_{T_i} can be calculated as

$$d_{\mathcal{H}}(D_S, D_{T_i}) = 2 \sup_{\mathcal{D} \sim \mathcal{H}} \left| \Pr_{x \sim D_S} [\mathcal{D}(x) = 1] - \Pr_{x \sim D_{T_i}} [\mathcal{D}(x) = 1] \right| \quad (7)$$

, where \mathcal{H} denotes hypothetical space and \mathcal{D} denotes discriminator. Similar to [19], due to our model without discriminator architecture, calculating the \mathcal{H} -divergence directly is challenging. For low-rank adapter evaluation, we adopt the *Jensen-Shannon (JS) divergence* between two adjacent domains as an approximation.

$$JS(P_{D_S} || P_{D_{T_i}}) = \frac{1}{2} KL(P_{D_S} || \frac{P_{D_S} + P_{D_{T_i}}}{2}) + \frac{1}{2} KL(P_{D_{T_i}} || \frac{P_{D_S} + P_{D_{T_i}}}{2}) \quad (8)$$

Where *Kullback-Leibler (KL) divergence* between two domain is

$$KL(P_1 || P_2) = \sum_{i=0}^n P_1(x_i) \log\left(\frac{P_1(x_i)}{P_2(x_i)}\right) \quad (9)$$

Where P denotes probability distribution of model output features. We split the output feature space into mutually disjoint intervals x_i . n range from 0 to 1000. To investigate the effectiveness of

adapters in adapting to continual target domains, we compare the JS values obtained by using the source model alone, injecting low-rank adapter, and combining low-high adapters, as illustrated in Figure 3(a) of our submission. For high-rank adapter, we use normalized intra-class divergence to further verify the domain representations of high-rank adapters in CIFAR10C, which is inspired by intra-cluster dissimilarity proposed by k -means [42]. We first calculate the Euclidean distance clustering center for each category $\mu = \frac{1}{|C|} \sum_{e_i \sim C} e_i$, where e_i stands for output feature in class C . Then following [42], we introduce normalized intra-class divergence E by

$$E = \phi\left(\frac{1}{|C|} \sum_{e_i \sim C} \|e_i - \mu\|_2^2\right) \quad (10)$$

$\phi(\cdot)$ denotes for normlization function. As illustrated in Figure 3(b) of the submission, the high-rank adapter is found to drive down divergence within almost all domains and can better extract domain-specific knowledge in target domains.

Distribution Quantitative Analysis To provide stronger evidence for our assumption, we have developed two evaluation approaches for both low-rank and high-rank adapters, which directly reflect their ability to extract domain-agnostic and domain-specific knowledge on ImageNet-to-ImageNet-C. After completing the entire process of continual adaptation on fifteen target domains, we employ the model and adapters from the last target domain to directly test on previously seen target domains, thereby evaluating the extent of catastrophic forgetting. As anticipated, we observe a noteworthy overall improvement of 1.0% in the average classification error, as demonstrated in the final row of Table 1 (submission). These findings provide additional support to our assumptions and indicate that utilizing low-rank adapters can mitigate catastrophic forgetting. Secondly, we conduct an ablation study on ImageNet-to-ImageNet-C to demonstrate the effectiveness of the high-rank adapter. In this study, we solely introduce the high-rank adapter into the pre-trained model. The results, presented in Table 6 (Ex_2) of the submission, reveal a sustained reduction (-4.6%) in the classification error rate within the dynamic target domains when employing the high-rank adapter. This finding provides support for our hypothesis that high-rank adapters can extract more dependable domain-specific knowledge. These evaluation approaches serve to strengthen our findings and contribute to a clearer understanding of the capabilities and advantages of both low-rank and high-rank adapters.

C Additional Experiment

C.1 Additional Continual Adaption Experiments for Foundation Models

Table 7: Average error rate (%) for the ImageNet-to-ImageNet-C CTTA task. All results are evaluated on the ViT-Base, which uses the pre-trained encoder parameter of DINOv2 [44] and SAM [33].

Backbone	Method	REF	Gaussian	shot	impulse	defocus	glass	motion	zoom	show	frost	fog	brightness	contrast	elastic_trans	pixelate	jpeg	Mean↓	Gain
DINOv2	Source		52.3	50.5	51.2	57.3	83.8	60.1	62.6	47.1	56.9	58.1	22.5	88.4	60.3	32.4	35.0	54.6	0.0
	Tent [58]	ICLR2021	51.7	43.6	50.4	56.2	74.1	51.7	67.2	46.9	53.2	50.1	25.2	69.6	58.0	29.5	39.4	51.1	+3.5
	CoTTA [59]	CVPR2022	51.4	62.1	50.4	78.3	75.2	62.8	60.3	48.4	59.0	58.8	31.6	90.7	49.2	39.1	36.5	56.9	-2.3
	Ours	Proposed	49.0	49.8	50.7	61.4	60.2	49.7	42.6	47.1	51.9	45.3	27.1	49.7	47.4	32.0	29.4	46.2	+8.4
SAM	Source		67.9	62.1	51.6	69.7	92.6	65.4	59.8	53.9	61.2	64.1	39.0	91.6	60.1	47.3	67.0	63.6	0.0
	Tent [58]	ICLR2021	67.2	59.1	48.8	56.2	72.5	59.4	61.0	49.1	57.9	63.7	33.8	77.0	51.4	39.5	55.2	55.5	+8.1
	CoTTA [59]	CVPR2022	68.1	64.5	50.4	67.1	80.1	68.9	67.0	63.1	69.5	61.4	40.6	88.2	58.3	43.5	68.4	63.9	-0.3
	Ours	Proposed	59.9	55.7	40.2	84.3	49.6	59.7	59.0	47.8	48.3	57.4	26.6	71.8	42.9	41.7	50.3	53.0	+10.6

To demonstrate the effectiveness of our proposed method in enhancing the continual adaptation ability of foundation models such as DINOv2 [44] and SAM [33], we conducted additional experiments on a more extensive dataset, namely ImageNet-to-ImageNet-C. Our approach involved loading the weight parameters of the foundation model and pre-training it on ImageNet, thus constructing our source model. It is important to note that we solely utilized the pre-trained encoder of SAM and incorporated a classification head, which was fine-tuned on the source domain. Subsequently, we adapted the source model to continual target domains (ImageNet-C) comprising fifteen corruption types. The results, as depicted in Table 7, demonstrate that our approach achieved a significant performance improvement of 8.4% on the representative image-level foundation model DINOv2 [44] and 10.6% on the pixel-level foundation model SAM [33]. These outcomes highlight the effectiveness of our

method when applied to large-scale models. Our method consistently and reliably enhances the performance of the foundation model across unseen continual target domains.

C.2 Domain Generalization on a Different Number of Unseen Target Domains

Table 8: We performed domain generalization comparisons on ImageNet-C, where the source model was continually adapted on the first 5 domains and directly tested on 10 unseen domains. The evaluation of the results was conducted using ViT-base.

Method	Directly test on 10 unseen domains										Unseen
	motion	zoom	snow	frost	fog	bri.	contrast	elastic_trans	pixelate	jpeg	Mean↓
Source	58.5	63.3	49.9	54.2	57.7	26.4	91.4	57.5	38.0	36.2	53.3
Tent [58]	56.0	61.3	45.7	49.6	56.6	24.8	94.0	55.6	37.1	35.1	51.6
CoTTA [59]	57.3	62.1	49.1	52.0	57.1	26.4	91.9	57.1	37.6	35.3	52.6
Ours	46.4	52.7	39.8	43.7	42.2	23.5	71.5	49.6	33.9	33.3	43.7

Table 9: We performed domain generalization comparisons on ImageNet-C, where the source model was continually adapted on the first 7 domains and directly tested on 8 unseen domains. The evaluation of the results was conducted using ViT-base.

Method	Directly test on 8 unseen domains								Unseen
	snow	frost	fog	bri.	contrast	elastic_trans	pixelate	jpeg	Mean↓
Source	49.9	54.2	57.7	26.4	91.4	57.5	38.0	36.2	51.4
Tent [58]	44.3	48.8	51.8	24.9	83.7	55.2	35.4	34.7	47.4
CoTTA [59]	48.8	52.2	56.7	26.1	91.1	57.0	37.3	35.3	50.6
Ours	39.6	43.7	41.7	23.7	63.7	51.7	33.3	33.6	42.3

Similar to our previous submission, we follow the leave-one-domain-out principle [65, 39], where we utilize a subset of ImageNet-C domains as new source domains for model training, while leaving the remaining domains as target domains without any adaptation. However, in contrast to previous domain generalization experiments, we adopt an unsupervised continual test-time adaptation (CTTA) approach for training the model on these new source domains. We solely utilize the ImageNet pre-trained parameters as the initial weights of the model. In the supplementary material, we utilize 5 out of 15 and 7 out of 15 domains from ImageNet-C as the source domains, leaving the remaining 10 out of 15 and 8 out of 15 domains as unseen target domains. Surprisingly, the results presented in Table 8 and 9 demonstrate that our method achieves a reduction of 9.6% and 9.1% in the average error on these unseen domains, respectively. These promising outcomes validate the DG ability of our method, as it effectively extracts domain-agnostic knowledge and provides a new perspective for enhancing DG performance within an unsupervised paradigm.

C.3 Additional Ablation study

How do the prototype dimension influence the performance?

According to Figure 5, we observe that as the dimensionality decreases, the error rate concurrently drops. This trend suggests that lower-dimension prototypes more effectively extract the domain-shared knowledge, leading to an improved model performance. However, an opposite trend emerges when dimensionality surpasses 16, with performance enhancements accompanying increased dimensionality. This correlation implies that prototypes with a higher dimensionality excel in extracting domain-specific knowledge. And we find that when the dimension is larger than 128, the performance improvement is limited but brings a larger number of parameters. Therefore, we set the dimensionality of the high-dimension prototype to 128 in our study.

C.4 Additional Experiments on Classification CTTA

CIFAR10-to-CIFAR10C standard task. In contrast to the experiments conducted in our submission, we introduce a change in the backbone of the classification model to WideResNet-28, which is consistent with previous works on CTTA [59]. Specifically, we modify the up-projection layer and down-projection layer to utilize 1×1 convolutions, while the adapters are placed alongside the

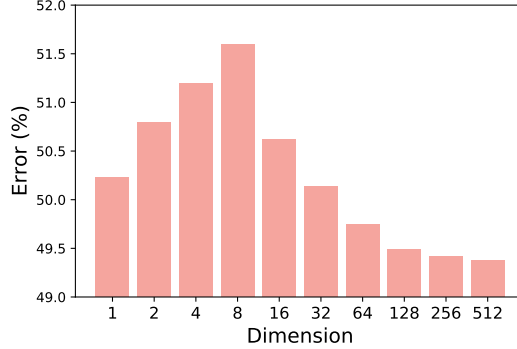


Figure 5: The prototype dimension influence of the performance

Table 10: Classification error rate(%) for standard CIFAR10-to-CIAFAR10C online CTTA task. Results are evaluated on WideResNet-28. Gain(%) represents the percentage of improvement in model accuracy compared with the source method.

Method	REF	Gaussian	shot	impulse	defocus	glass	motion	zoom	snow	frost	fog	brightness	contrast	elastic_trans	pixelate	jpeg	Mean↓	Gain
Source [63]	BMVC2016	72.3	65.7	72.9	46.9	54.3	34.8	42.0	25.1	41.3	26.0	9.3	46.7	26.6	58.5	30.3	43.5	0.0
BN Stats Adapt [52]	NeurIPS2020	28.1	26.1	36.3	12.8	35.3	14.2	12.1	17.3	17.4	15.3	8.4	12.6	23.8	19.7	27.3	20.4	+23.1
Tent-continual [58]	ICLR2021	24.8	20.6	28.6	14.4	31.1	16.5	14.1	19.1	18.6	18.6	12.2	20.3	25.7	20.8	24.9	20.7	+22.8
CoTTA [59]	CVPR2022	24.3	21.3	26.6	11.6	27.6	12.2	10.3	14.8	14.1	12.4	7.5	10.6	18.3	13.4	17.3	16.2	+27.3
SATA [8]	2023.4.20	23.9	20.1	28.0	11.6	27.4	12.6	10.2	14.1	13.2	12.2	7.4	10.3	19.1	13.3	18.5	16.1	+27.4
Ours	Proposed	24.1	20.6	24.1	11.5	26.5	12.3	10.3	14.7	13.4	12.3	8.3	10.9	17.7	12.9	16.8	15.8	+27.7

original 3×3 convolutions. For the adapters, we maintain a low-rank dimension of 1 and a high-rank dimension of 128. Additionally, we provide the pre-trained source model and perform CTTA on CIFAR10C, a dataset that encompasses fifteen corruption types that occur sequentially during the test time. As depicted in Table 10, our method surpasses all previous approaches, achieving a 27.7% and 0.3% improvement over the source model and the previous state-of-the-art (SOTA) method. These findings demonstrate that our method successfully extracts domain-specific knowledge, regardless of the network backbone employed.

D Additional Qualitative Analysis

To further validate the effectiveness of our proposed method, we present additional qualitative comparisons on the Cityscapes-to-ACDC CTTA scenario. Initially, we pre-train the Segformer-B5 model [60] on the source domain and subsequently adapt it to four target domains in ACDC. In order to assess the performance of our approach, we conduct a qualitative comparison with two leading methods, namely CoTTA [59] and VDP [17]. The visualizations of the segmentation outputs, obtained through the CTTA process, are depicted in Figure .6. Our method exhibits better segmentation map compared to CoTTA and VDP across all four target domains, as it effectively distinguishes the sidewalk from the road (shown in white box). This demonstrates the capability of our method to achieve more accurate segmentation results while mitigating the impact of dynamic domain shifts. Moreover, in the other categories, our method’s segmentation maps closely resemble the Ground Truth, leading to a visual enhancements. Lastly, we have included a video visualization in the supplementary material that showcases a comprehensive comparison of segmentation performance. This video provides a dynamic and visual representation of the results obtained from our experiments.

E Additional Related Work

E.1 Continual Test-Time Adaptation

Test-time adaptation (TTA), also known as source-free domain adaptation [6, 35, 41, 62], aims to adapt a source model to an unknown target domain distribution without relying on any source domain data. In practical scenarios where data privacy and transmission costs are a concern, access

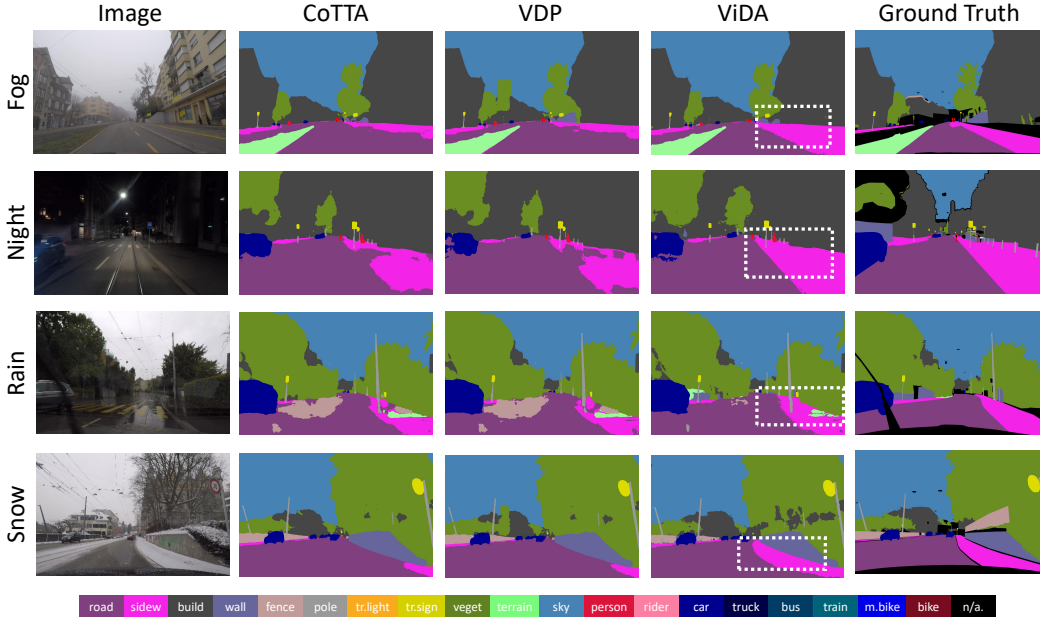


Figure 6: Qualitative comparison of our method with previous SOTA methods on the ACDC dataset. Our method could better segment different pixel-wise classes such as shown in the white box.

to source domain data may be limited, rendering traditional unsupervised domain adaptation (UDA) algorithms ineffective. Recent research has explored various techniques such as self-training and entropy regularization to fine-tune the source model [36, 58, 41, 9]. Specifically, Tent [58] updates the training parameters in batch normalization layers by minimizing entropy. SHOT [41] focuses on optimizing only the feature extractor using information maximization and pseudo-labeling. AdaContrast [9] combines pseudo-labeling with self-supervised contrastive learning to improve performance. Additionally, some studies have approached the problem from an output distribution adjustment perspective [7]. Recently, SVDP introduces the sparse domain prompt to address the pixel-level domain shift for segmentation TTA task. While the works mentioned above primarily concentrate on convolutional neural networks, there has been a recent surge of interest in applying Transformer-based models [59, 21, 21].

Continual Test-Time Adaptation (CTTA) refers to a scenario where the target domain is dynamic, presenting additional challenges for traditional TTA methods. The pioneering work by [59] introduced a comprehensive approach that combines bi-average pseudo labels and stochastic weight reset to address this complex task. While [59] focuses on tackling the problem at the model level for both classification and segmentation tasks, [17] proposes the use of visual domain prompts at the input level, specifically for the classification task. In a similar vein, inspired by Tent [58], SATA [8] modifies the batch-norm affine parameters through a source anchoring-based self-distillation scheme. Building upon these advancements, our paper takes a pioneering step by introducing visual domain adapters to address the challenges of error accumulation and catastrophic forgetting in CTTA. By simultaneously tackling both classification tasks and dense prediction tasks, our approach provides a holistic solution for CTTA.

E.2 Parameter-Efficient Fine-Tuning

Selective updating or introducing a small subset of parameters instead of updating all parameters in a pre-trained model during standard fine-tuning has been shown to be effective. In the field of natural language processing (NLP), Parameter-Efficient Fine-Tuning (PEFT) has gained considerable traction, with notable studies including [31, 27, 26, 64, 38, 28, 20, 24, 56, 46]. Adapter-based models, a type of PEFT, have emerged as popular techniques in NLP. These models utilize bottleneck architecture adapter modules that are inserted between layers of pre-trained models, and during fine-tuning, only these adapter modules are updated. Adapter-based models have demonstrated superior performance in certain tasks, sometimes surpassing standard fine-tuning approaches [13]. The success of adapters

in NLP has also led to widespread interest in applying adapter techniques to visual tasks. During the early stages of adapter development, residual adapter modules were introduced as a means to facilitate effective adaptation of convolutional neural networks across multiple downstream tasks [47, 48]. Building on this foundation, AdaptFormer [11] improves the ViT [15] model by replacing the original multi-layer perceptron (MLP) block with AdaptMLP. AdaptMLP introduces a trainable down-to-up bottleneck module in a parallel manner, effectively mitigating catastrophic interference between tasks. Another notable approach, VL-Adapter [53], enhances the efficiency and performance of adapters by leveraging shared low-dimensional layer weights to transfer knowledge across tasks. Despite these advancements, existing methods have not adequately addressed the challenges of long-term preservation of domain-agnostic knowledge and the timely exploration of domain-specific knowledge in the face of continuous unknown domain variations. Consequently, there is an urgent demand for an adapter that can simultaneously address the challenges of error accumulation and catastrophic forgetting through specific adapters with different domain representations.

F Fine-grained Performance

Table 11: A fine-grained Classification error rate(%) for standard CIFAR10-to-CIFAR10C online CTTA task. Results are evaluated on ViT-base.

Method	gaussian	shot	impulse	defocus	glass	motion	zoom	snow	frost	fog	bri.	contrast	elastic_trans	pixelate	jpeg	Mean↓	Gain
Source	60.1	53.2	38.3	19.9	35.5	22.6	18.6	12.1	12.7	22.8	5.3	49.7	23.6	24.7	23.1	28.2	0.0
Pseudo-label [37]	59.8	52.5	37.2	19.8	35.2	21.8	17.6	11.6	12.3	20.7	5.0	41.7	21.5	25.2	22.1	26.9	+1.3
Tent-continual [58]	58.7	51.8	34.2	18.9	33.5	21.6	16.4	10.8	11.7	18.6	4.7	38.5	20.6	22.1	20.8	25.5	+2.7
CoTTA [59]	58.7	51.3	33.0	20.1	34.8	20	15.2	11.1	11.3	18.5	4.0	34.7	18.8	19.0	17.9	24.6	+3.6
VDP[17]	57.5	49.5	31.7	21.3	35.1	19.6	15.1	10.8	10.3	18.1	4	27.5	18.4	22.5	19.9	24.1	+4.1
Ours (proposed)	52.9	47.9	19.4	11.4	31.3	13.3	7.6	7.6	9.9	12.5	3.8	26.3	14.4	33.9	18.2	20.7	+7.5

Table 12: A fine-grained Classification error rate(%) for standard CIFAR100-to-CIFAR100C online CTTA task. Results are evaluated on ViT-base.

Method	gaussian	shot	impulse	defocus	glass	motion	zoom	snow	frost	fog	bri.	contrast	elastic_trans	pixelate	jpeg	Mean↓	Gain
Source	55.0	51.5	26.9	24.0	60.5	29.0	21.4	21.1	25.0	35.2	11.8	34.8	43.2	56.0	35.9	35.4	0.0
Pseudo-label [37]	53.8	48.9	25.4	23.0	58.7	27.3	19.6	20.6	23.4	31.3	11.8	28.4	39.6	52.3	33.9	33.2	+2.2
Tent-continual [58]	53.8	48.7	25.5	23	59.1	27.4	19.7	20.9	23.5	31.8	11.8	27.9	39.9	50.9	33.8	33.2	+2.2
CoTTA [59]	55.0	51.3	25.8	24.1	59.2	28.9	21.4	21.0	24.7	34.9	11.7	31.7	40.4	55.7	35.6	34.8	+0.6
VDP [17]	54.8	51.2	25.6	24.2	59.1	28.8	21.2	20.5	23.3	33.8	7.5	11.7	32.0	51.7	35.2	32.0	+3.4
Ours (proposed)	50.1	40.7	22.0	21.2	45.2	21.6	16.5	17.9	16.6	25.6	11.5	29.0	29.6	34.7	27.1	27.3	+8.1

In this section, we expand upon the classification results presented in our submission by providing a details of fine-grained performance. We assess the error rates across fifteen corruption types to gain deeper insights. To be specific, we augment the information provided in Table 2 of our submission with the additional details presented in Table 11 and 12. These tables offer a comprehensive view of the performance of our approach in addressing the CIFAR-10-to-CIFAR-10C and CIFAR-100-to-CIFAR-100C CTTA scenarios, respectively.